Dynamic Characteristics of Rotors on Passive and Active Thrust Fluid-film Bearings with Fixed Pads

Alexander Babin[1,*], *Leonid* Savin[1], and *Sergey* Majorov[1]

[1] Dept. of Mechatronics, Mechanics and Robotics, Orel State University, Naugorskoe sh. 29, 302020, Orel, Russia

Abstract. Application of fluid-film bearings in rotor machines in many cases could have no alternative due to obvious advantages when compared to roller element bearings. Integration of information technology in mechanical engineering resulting in emergence of a new field of research – mechatronic bearings which allowed tracking condition of the most important parts of a machine and adjusting operational parameters of the system. Application of servo valves to control the flow rate through a fluid-film bearing is the most universal and simple way of rotor's position control due to relative simplicity of modelling and absence of need to radically change the design of conventional hydrodynamic bearings. In the present paper numerical simulations of passive (conventional as opposed to mechatronic) and active hybrid thrust fluid-film bearings with a central feeding chamber are presented, that are parts of a mechatronic rotor-bearing node. Numerical model of an active thrust bearing is based on solution of equations of hydrodynamics, rotor dynamics and an additional model of a servo valve. Various types of control have been investigated: P, PI and PID control, and the dynamic behaviour of a system has been estimated under various loads, namely static, periodic and impulse. A design of a test rig has been proposed to study passive and active thrust fluid-film bearings aimed at, among other, validation of numerical results of active bearings simulation.

1 Introduction

Investigation in the field of rotor's dynamic behaviour control in fluid-film bearings is carried out in the following fields: study of the possibility of profile adjustment of a gap between a rotor and a sleeve or a thrust disk of a bearing, e.g. tilting-pad and some foil bearings [1, 2]; study of the possibility of application of lubricants with adjustable parameters such as viscosity or density, e.g. ferromagnetic fluids [3, 4]; and study of hybrid fluid-film bearings [5, 6], where load capacity is generated as a combination of hydrodynamic forces in the film and hydrostatic force from the lubricant supplied into a bearing under pressure, where rotor's position can be adjusted by means of electrohydraulic devises like servo valves.

Application of servo valves to control the flow rate through a bearing is the most universal and simple way of rotor's position control due to relative simplicity of modeling and absence of need to radically change the design of conventional hydrodynamic bearings. However, the field of active hybrid bearings is not as investigated, as, for instance, magnetic bearings. Despite the fact, that fluid-film bearings with additional elements to form a control system are significantly cheaper than the magnetic bearings with complex structure and maintenance, the modelling of them requires a lot of numerical tests to solve the design problems. Both thrust and journal fluid-film bearings are used in industrial applications, such as centrifugal pumps, that extrude crude oil, and bearings in them are lubricated with the same medium they extrude. The fields of application also include turbo generators, rockets, etc. In every case, a unique set of operational parameters dictates the design of a bearing.

In the present paper numerical simulations of passive (conventional as opposed to mechatronic) and active hybrid thrust fluid-film bearings with a central feeding chamber are presented, that are parts of a mechatronic rotor-bearing node.

2 Numerical simulations of passive hybrid thrust fluid-film bearings

In the present paper, a fixed-pad type of a hybrid thrust fluid-film bearing is considered. This type is the easiest to manufacture and requires no complications of a model, as opposed to, for instance, tilting pad thrust bearings. For further clarification, in this case 'hybrid' stands for a combination of hydrodynamic lifting force, generated due to the lubricant being dragged into the converging gap between a fixed pad and the rotor's disk, and hydrostatic lifting force, generated by the lubricant being supplied to the axial gap under pressure. Numerical simulations of passive hybrid thrust bearings (PHTB) are a base for further modelling of active hybrid thrust bearings (AHTB), the conceptual model of which is described below.

* Corresponding author: alex.mech.osu@gmail.com

2.1. Conceptual model of an ATHB

The operational principle of an ATHB (Figure 1) is as follows: the pump (1), located in the tank with the fluid (water, oil, etc.), supplies the lubricant into the housing (2) of the bearing (3), which supports the rotor (4) in the axial direction. The pressure data is acquired with the sensor (8). The data on the present position of the rotor is acquired with the proximity sensor (7). Data from the sensors is analogue and is acquired with the analogue input modules of a DAQ system (5). This system also controls the servovalve (6) by means of adjusting the opening rate ξ generating an analogue voltage signal, and the pump (descrete output module).

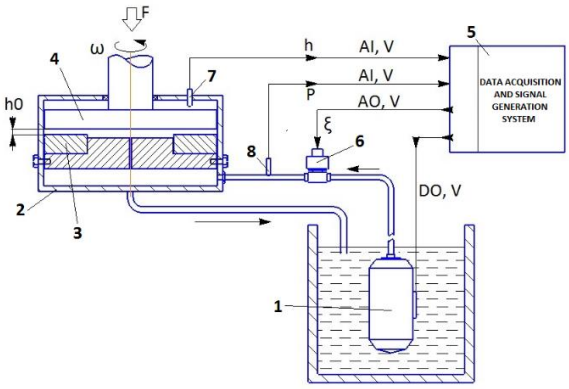

Fig. 1. Conceptual model of an AHTB.

2.2 Basic equations of PHTBs modelling

To simulate the operation of a rotor on a PHTB, one has to determine the reaction forces of the lubricant film, thus being able to obtain dynamic coefficients, i.e. stiffness and damping, to simulate the rotor's dynamic behaviour.

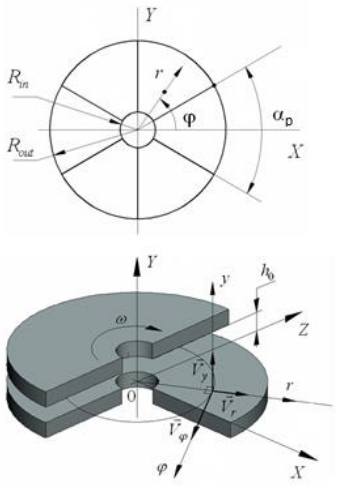

Fig. 2. Calculation diagram of a PHTB.

The first step in this modelling is determination of pressure distribution over the surface of the rotor's disk, which is governed by the Reynolds equation in polar coordinates in accordance to the diagram in the Figure 2:

$$\frac{\partial}{\partial\varphi}\left[\frac{\Phi_\varphi h^3}{rK_\varphi\mu}\frac{\partial p}{\partial\varphi}\right]+\frac{\partial}{\partial r}\left[\frac{\Phi_r h^3}{K_r\mu}\frac{\partial p}{\partial r}\right]= \\ =6\omega r\frac{\partial h}{\partial\varphi}+6\omega r\sigma\frac{\partial\Phi_s}{\partial\varphi}+12V_y, \quad (1)$$

where Φ_r, Φ_φ and Φ_s – radial, circumferential pressure and shear flow rate coefficients accordingly, which are determined as described in [7,8], h – axial gap function, K_φ and K_r – viscosity coefficients determined according to [9], p – pressure, μ - dynamic viscosity of the lubricant and is a function of temperature: $\mu=\mu_{in}e^{-\lambda(T-T_s)}$, λ – temperature/viscosity coefficient, μ_{in} – viscosity of the supplied medium, T_s – temperature of the supplied lubricant, ω – angular speed of the shaft, σ – RMS roughness of the surfaces of the rotor's, V_y – velocity of the shaft in the direction of film thickness.

The solution of (1) in the present case requires the following boundary conditions for a single pad:

$$p\big|_{r=Rout}=p_a,\ p\big|_{r=Rin}=p_s,$$
$$p\big|_{\varphi=0}=p\big|_{\varphi=\alpha_p},\ \left.\frac{\partial p}{\partial\varphi}\right|_{\varphi=0}=\left.\frac{\partial p}{\partial\varphi}\right|_{\varphi=\alpha_p},$$

where p_a – ambient pressure, p_s – supplied pressure, i.e. pressure in the feeding chamber, α_p – angular extent of a single pad.

The pressure distribution in a fluid is greatly influenced by the temperature of the fluid and the surrounding surfaces. The temperature distribution is governed by the energy equation, which in many cases has to be solved for a three-dimensional flow. However, for relatively low rotational speeds as shown in [10] a two-dimensional energy equation gives a quite accurate results. The energy equation for the present case is as follows:

$$\rho c_p\left(-\frac{h^2}{12\mu}\frac{\partial p}{\partial r}\frac{\partial T}{\partial r}+\left(-\frac{h^2}{12\mu r}\frac{\partial p}{\partial\varphi}+\frac{\omega r}{2}\right)\frac{\partial T}{r\partial\varphi}\right)= \\ =\mu\left(\left(\frac{1}{12}\left(\frac{h}{\mu}\frac{\partial p}{\partial r}\right)^2\right)+\left(\frac{1}{12}\left(\frac{h}{\mu}\frac{\partial p}{r\partial\varphi}\right)^2+\left(\frac{\omega r}{h}\right)^2\right)\right), \quad (2)$$

where ρ – fluid's density, c_p – specific heat of the fluid, T – temperature.

The solution of (2) requires the following boundary conditions:

$$T\big|_{r=Rin}=T_s,$$
$$T\big|_{\varphi=0}=T\big|_{\varphi=\alpha_p},$$
$$\left.\frac{\partial T}{\partial\varphi}\right|_{\varphi=0}=\left.\frac{\partial T}{\partial\varphi}\right|_{\varphi=\alpha_p},$$

where T_s – temperature of the supplied lubricant.

Numerical solution of (1) and (2) yields pressure and temperature distribution over the surface of the rotor's disk. The procedure is implemented in a series of iterations until a load capacity convergence accuracy is achieved. Equations (1) and (2) are solved using the finite difference method.

2.3 Static characteristics of PTHBs

Determination of static characteristics, namely load capacity R_Y, friction torque M_{FR} and power loss due to friction N_{FR} being of the most significance in this case, is a further step in modelling the dynamic behaviour of the rotor. These characteristics are determined by means of integration of the pressure distribution:

$$R_Y = z \int_{Rin}^{Rout} \int_{0}^{\alpha_p} p r d\varphi dr,$$

$$M_{FR} = r \int_{Rin}^{Rout} \int_{0}^{\alpha_p} \left[\frac{h}{2} \frac{\partial p}{r \partial \varphi} + \frac{\omega r \mu K_\varphi}{h} \right] r d\varphi dr,$$

$$N_{FR} = M_{TP} \omega,$$

where z – number of pads.

In the Figure 3 and the Figure 4 the results of calculation of axial force R_Y and power loss due to friction accordingly depending on the minimum film thickness for various pad inclination angles are presented. For the Figure 3 the following modelling parameters were used : *Rout* = 0.06 m, *Rin* = 0.03 m, lubricant – H_2O @ 23ºC , ω = 900 rad/s, $\sigma_{pad,\ rotor}$ = 5µm. For the Figure 4 the following modelling parameters were used : *Rout* = 0.06 m, *Rin* = 0.03 m, lubricant – H_2O @ 23ºC, ω = 900 rad/s
$\sigma_{\text{pad, rotor}}$ = 5µm, α = 0.25º.

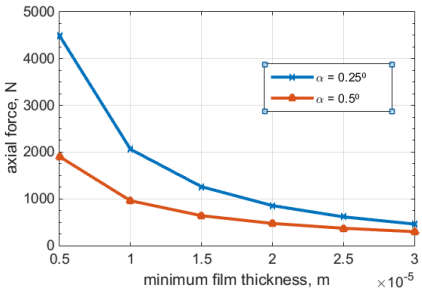

Fig. 3. Axial force of a PHTB versus minimum film thickness.

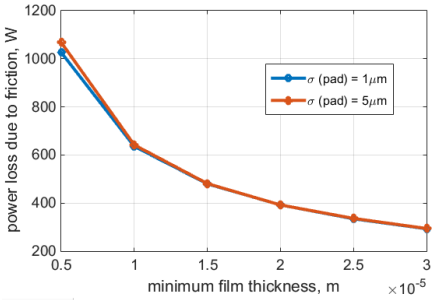

Fig. 4. Power loss due to friction versus minimum film thickness.

From these results one could tell, that geometry plays a big role in providing energy efficient operation with sufficient load capacity, which is crucial for most of the rotor machines. Additionally, when the fluid film is very thin, if, for instance, the load is high or the speed is low, one could notice the influence of the pads' roughness on the power loss due to friction. This leads to the necessity of high precision during the mechanical treatment of the parts of various machines and additional simulations in every particular case of operational conditions.

2.3 Static characteristics of PTHBs

Determination of dynamic characteristics requires representation of the rotor-bearing node as shown in the Figure 5.

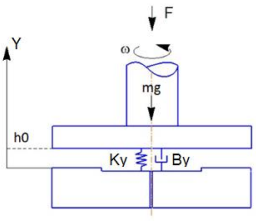

Fig. 5. Rotor-bearing dynamic system.

The present step of modelling aims at determination of stiffness and damping coefficients of the bearings, K_Y and B_Y accordingly.
Under steady conditions the rotor takes the equilibrium position, when the hydrodynamic forces counterbalance the inertia forces, i.e. $R_{Y0} = mg$, where m – rotor's mass, g – freefall acceleration. When the rotor's position changes under the influence of some impulse, some additional forces start acting on the rotor, so, assuming these displacements are relatively small, the reaction force of a bearing could be linearized using Taylor series. The reaction force of the bearing could be determined as follows:

$$R_y = R_{Y0} - K_Y \Delta Y - B_Y \Delta \dot{Y},$$

and, consequently, the motion law of the system is as follows:

$$m\ddot{Y} - B_Y \dot{Y} - K_Y Y = F(t),$$

where $F(t)$ is some external force as a function of time t.

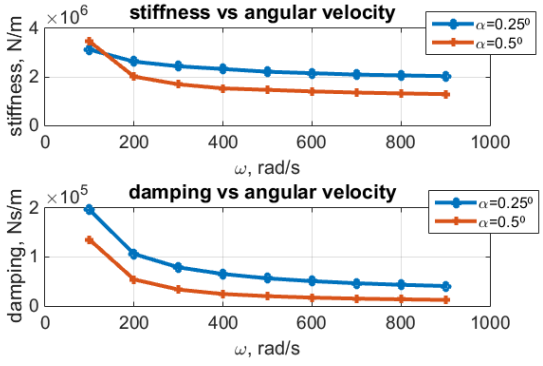

Fig. 6. Stiffness and damping of a PHTB versus angular velocity.

In the Figure 6, the results of the simulations show, how stiffness and damping of the PHTB are influenced by the angular velocity for various inclination angles of a single pad. The following modelling parameters were used: *Rout* = 0.06 m, *Rin* = 0.03 m, lubricant – H_2O @ 23^{0}C, σ_{pad}= 2.4 μm, $\sigma_{rotor}\approx$ 0 μm, mass of the rotor – 5.5 kg.

It could be seen, that for most of the operational conditions both stiffness and damping are higher for lower inclination angles of the pad, which could be explained by the fact, that with lower inclination angles the area of the pad where pressure is generating the load capacity is bigger, thus increasing the dynamic characteristics.

For further simulations the following types of the external loading are modelled: zero external load, periodic external load of 30 N at approx. 8 Hz, static load of 30 N and impulse load of 30 N applied in the middle of modelling time. The resulting rotor trajectories are presented in the Figure 7.

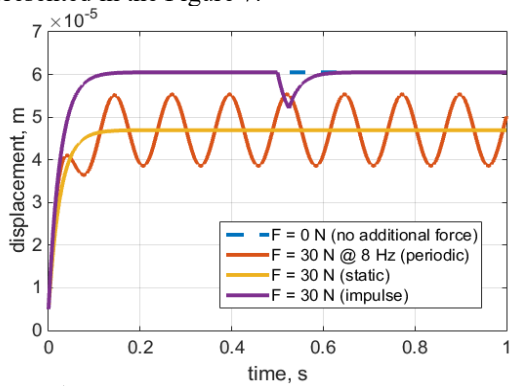

Fig. 7. Trajectories of the rotor with different loads.

3 Numerical modelling of AHTBs

According to the Figure 1, in the present case the active control of rotor's axial displacement is implemented by means of application of a servo valve. This kind of electrohydraulic actuators is simulated using the known relation between the pressure it supplies the lubricant with and the voltage on the input of the valve. The most important term here is the time constant of the valve T_{SV}, i.e. the time it takes for a fully closed valve to fully open. This is a crucial characteristic for systems subjected to high-frequency periodic loads.

The expression that allows simulation of a servo valve is as follows:

$$T_{SV}\frac{dp(t)}{dt}+p(t)=K_{SV}u(t),$$

where K_{SV} – gain coefficient of a servo valve, $u(t)$ – control signal, i.e. voltage on the servo valve's input.

Operation of the control system introduced to a PHTB significantly influences the stability of the system. It is possible to see how rotor's displacement is influenced depending on the simulated servo valve arbitrarily setting the time constant to various settings. Such comparison is shown in the Figure 8.

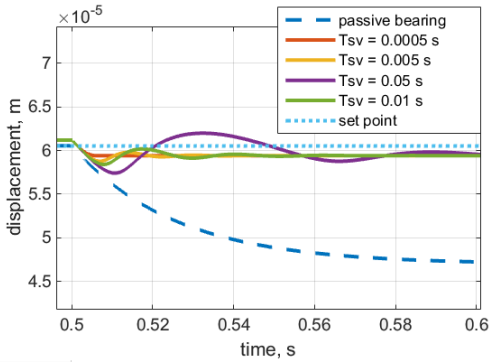

Fig. 8. Trajectories of the rotor depending on the time constant of a servo valve.

The set point value is in this case chosen to be the equilibrium position of the rotor on a PHTB. The simulated load was applied in the middle of the calculated time, and it could be seen from the Figure 8, that depending on the value of T_{SV} the control system affects the rotor's position differently in terms of induced oscillations. At this stage, it becomes obvious, that the choice of an actuator for specific application is indeed a very important task, especially if a system is subjected to high frequency vibrations or chaotic impacts of external nature.

In the light of this fact, it is also necessary to see how the controller setting influence the dynamic coefficients of stiffness and damping of a bearing. In the Figure 8 the simulation results are presented for a case of an AHTB under static load applied in the middle of the simulation time.

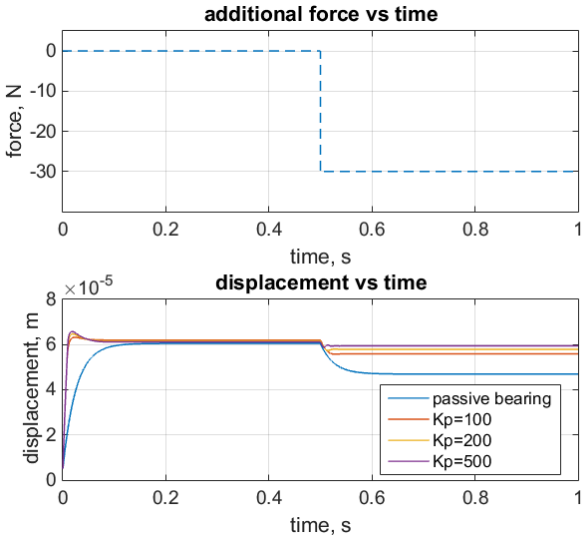

Fig. 8. Trajectories of the rotor on an AHTB under static load

The modelling parameters are as follows: ω = 500 rad/s, *Rout* = 0.06 m, *Rin* = 0.03 m, lubricant – H_2O @ 23^{0}C, σ_{pad}= 2.4 μm, $\sigma_{rotor}\approx$ 0 μm, mass of the rotor – 5.5 kg, additional force = 30 N @ 0.5 s, T_{SV} = 0.005 s.

Various arbitrarily set values of the proportional coefficient were chosen in order to see the influence of the *Kp* on the rotor's dynamic behaviour. Primary objective here was to compare the stiffness coefficients.

For a passive bearing, the stiffness coefficient is approx. $2.2 \cdot 10^6$ N/m, while for an active bearing, stiffness increases accordingly with the increase of proportional coefficient *Kp* of a P-controller (Table 1).

Table 1. Comparison of the stiffness coefficients.

Proportional coefficient *Kp*	**Stiffness, N/m**
0 (passive bearing)	$2.2 \cdot 10^6$
100	$4.9 \cdot 10^6$
200	$8.1 \cdot 10^6$
500	$16.7 \cdot 10^6$

Application of active control based on P-, PI- and PID control could significantly reduce the amplitude of rotor's oscillations. The simulation results in the Figure 9 below show the behaviour of the modelled system under the influence of a periodic external force with various settings of a control system.

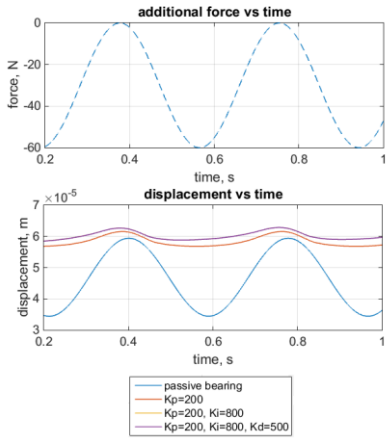

Fig. 9. Trajectories of the rotor on an AHTB under periodic load

Increase of the *Kp* of a P-controller allows decreasing of the oscillation amplitude, however a constant control error remains. Introduction of the *Ki* in a PI-controller appears to not have any significant influence. Addition of the *Kd* in a PID-controller allows this error to be decreased quite rapidly, the higher the setting, the faster the amplitude reaches values close to zero.

4 Results and discussion

Presented mathematical model allows evaluation of the influence of the control system based on an electrohydraulic device on the dynamic behavior of a rotor on an active thrust fluid-film bearing with fixed pads. Presented results show the importance of a careful choice of a servo valve, characteristics of which must meet the requirements of a particular application. Peculiarity of the presented type of control has been discovered: 'single-side' control only allows adjustment of the rotor's position below the set point, while decrease of the supplied pressure does not allow momentary adjustment of the position due to the properties of the lubricant and inertia properties of the rotor. This could be possibly avoidable by means of development of specific control algorithms or introduction of an additional hydraulic supply tract. Insignificance of *Ki* has been discovered, probably, due to small values of displacements (10^{-6} order of magnitude).

A test rig is being manufactured to verify the presented results and possibly to identify effects which occur and need to be taken into account. The schematic design of the rig is presented in the Figure 10.

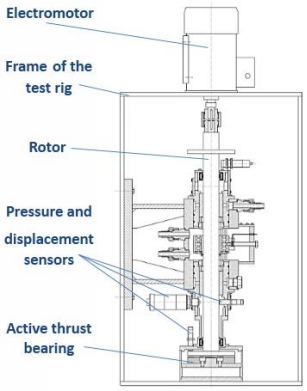

Fig. 10. Design of the test rig to study the AHTBs

The present research has been implemented as a part of the Russian Science Foundation project No. 16-19-00186 and Ministry of Education and Science of the Russian Federation project No. 9.2952.2017/4.6.

References

1. A. M. Haugaard, I. F. Santos, *Proceedings of the STLE/ASME International Joint Tribology Conference*, pp. 335–337 (2008)
2. G. Aguirre, F. Al-Bender, H. Van Brussel *PROCEEDINGS OF ISMA*, pp. 105-118 (2008)
3. H. Urreta, Z. Leicht, *Journal of Physics Conference Series,* **149** (2009)
4. A. Yu. Albagachiev, V.D. Danilov, *Bulletin of the Bryansk State Technical University,* **3**. pp. 90-93 (2016)
5. P. Kytka, B. Riemann, R. Nordmann, *Proceedings of the 9th International Conference on Motion and Vibration Control*, (2000)
6. L.A. Savin, S.V. Mayorov, D.V. Shutin, A.Y. Babin, *Proceedings of ICMMR MATEC Web of Conferences* **77**, 5 (2016)
7. N. Patir, H. S. Cheng, *ASME J. Lubr. Technol.*, **100**, pp. 12–17 (1978)

8. N. Patir, H. S. Cheng, *ASME J. Lubr. Technol*., **101**, pp. 220–229 (1979)
9. N. Tepey, V.N. Constantinescu, *Publishing House of the Academy of Sciences of the RNR*, 458 p. (1964)
10. I. Chatzisavvas, A. Boyaci, A. Lehn, M. Mahner, B. Schweizer, P. Koutsovasilis, *Proceedings of ASME Turbo Expo 2016: Turbomachinery Technical Conference and Exposition,* 10 p. (2016)